



Research paper

Reactivity of platform molecules in pyrolysis oil and in water during hydrotreatment over nickel and ruthenium catalysts

Chiara Boscagli^a, Klaus Raffelt^{a,*}, Jan-Dierk Grunwaldt^{a,b}^a Karlsruhe Institute of Technology, Institute of Catalysis Research and Technology, Hermann-von-Helmholtz-Platz 1, 76344, Eggenstein-Leopoldshafen, Germany^b Karlsruhe Institute of Technology, Institute for Chemical Technology and Polymer Chemistry, Engesserstr. 20, 76131, Karlsruhe, Germany

ARTICLE INFO

Article history:

Received 27 April 2017

Received in revised form

1 August 2017

Accepted 9 August 2017

Available online 30 August 2017

Keywords:

Biomass

Hydrodeoxygenation

Pyrolysis

Nickel catalyst

Hydrotreating

ABSTRACT

Hydrodeoxygenation (HDO) of fast pyrolysis oils for fuel and chemical production was investigated in a batch autoclave at 340 °C (8.0 MPa H₂ at room temperature) over nickel-based catalysts and Ru/C. The deoxygenation degree was similar over all catalysts, but different H/C ratios were observed in the upgraded oils, in line with the corresponding H₂ consumption. The highest values were found for Ru/C followed by NiCu/Al₂O₃. The composition of the upgraded oils produced over Ni-catalysts showed high ketone content, while the upgraded oil over Ru/C contained hydrocarbons and alcohols. Phenolic compounds exhibited low conversion over all catalysts. Subsequently the influence of the reaction medium (bio-oil or water) on the activity and selectivity of the catalyst was probed using phenol and D-glucose as model compounds representative for the cellulose and lignin fraction, respectively. Their reactivity in the bio-oil was tracked using isotopically-labelled phenol-d₆ and D-glucose-¹³C₆. Phenol was HDO resistant, while D-glucose formed a complex product mixture recovered in the upgraded oil. In aqueous solution, phenol was converted mainly to methane over Ru/C and cyclohexane over NiCu/Al₂O₃, whereas both catalysts promoted hydrocracking of D-glucose to methane. Comprehensive analysis of the spent catalysts showed that inorganic deposits and further components in the bio-oil lead to different reactivity in the two media.

© 2017 The Authors. Published by Elsevier Ltd. This is an open access article under the CC BY-NC-ND license (<http://creativecommons.org/licenses/by-nc-nd/4.0/>).

1. Introduction

The increasing scarcity of crude-oil reserves is driving a transition in the future energy economy from fossil to renewable resources. As the main renewable source of carbon, biomass is an attractive prospect for production of transport fuels and chemicals [1]. The main challenge of the last decades has been the utilization and valorization of lignocellulosic materials that are not in competition with food supply [2]. From an economic and energetic point of view, fast pyrolysis followed by an upgrading method is considered to be an attractive strategy [3] for producing a substrate that could be further co-processed in a refinery or converted to fuels/chemicals in dedicated facilities [4]. Fast pyrolysis is a versatile process for different biomass feedstocks and an easy solution for energy densification in volume [5]. However, the bio-oils produced are not directly suitable as transportation fuel or for chemical

production and a subsequent upgrading process is therefore necessary [3,5–10].

Hydrodeoxygenation (HDO) is usually the preferred method among upgrading processes (e.g. zeolite cracking) since it can produce high quality fuels with high carbon efficiency [3]. Using an appropriate HDO catalyst and high hydrogen pressure, oxygen is eliminated from the organic molecules in bio-oil in the form of water, producing an upgraded oil that is more stable, with higher heating value and more similar to crude oil. A lot of progress regarding HDO has been achieved in the last years, using hydrodesulfurization and noble metals catalysts [3]. However, improving long-term stability of the catalyst is still a prerequisite for industrial applications [11–14]. Recent efforts in HDO have focused on alternative catalysts [15], which are preferably sulfur free, economically viable and environmentally friendly. Especially nickel-based catalysts, which are also studied in this work, have attracted considerable interest [15–27].

Until now, most studies on HDO catalysts concern model compounds (reviews of Ref. [12,28]) rather than pyrolysis oils [3,8,16–19,29] and only a few comparisons between these two

* Corresponding author.

E-mail address: klaus.raffelt@kit.edu (K. Raffelt).

cases have been reported [17,30–32]. Testing a catalyst with model compounds presents the advantage of studying an easier system than bio-oils, which are difficult to compare with other literature studies due to their variable and complex composition. However, different factors that could affect the conversion and selectivity of a compound during HDO in pyrolysis oil, are generally not considered in studies with model compounds. For example, the polarity of the reaction medium [33], competitive adsorption of different species on the catalyst surface [32,34], parallel side-reactions [35] and catalyst deactivation [36–38] can lead to formation of different products, depending on whether the catalyst is tested in a pure solvent or in bio-oil.

The present work aimed to comprehend and compare the reactivity of phenol and D-glucose as platform molecules during HDO in pyrolysis oil and in a pure solvent. The light phase of a pyrolysis oil produced from wheat straw in the bioliq[®] pilot plant [39] was used, since it constitutes a simplified system for detecting reaction paths in comparison to the whole bio-oil. Firstly, the light phase was hydrotreated at 340 °C over different nickel-based catalysts (supported on different materials) and Ru/C (used as benchmark), and the catalyst performance and the reaction products were compared. Subsequently, the reactivity of isotopically-labelled compounds (phenol-d₆ and glucose-¹³C₆) in pyrolysis oil was monitored over NiCu/Al₂O₃ (as representative of Ni-catalyst class) and Ru/C and compared to their reactivity in pure water to further understand the influence of the bio oil on the conversion and selectivity of the catalysts.

2. Materials and methods

2.1. Pyrolysis oil, reagents and catalysts

The deep HDO carried out in this study is the extension of a previous work done at milder conditions (250 °C) reported in Ref. [40]. The same feed and catalysts were used. The feed was the light phase of a pyrolysis oil produced by wheat straw at the bioliq[®] plant at the Karlsruhe Institute of Technology. The light phase was produced by a spontaneous phase separation of the whole bio-oil after the production and contained 56.7% water and low molecular weight compounds, mainly sugar derivatives (details on the solvent fractionation are given in Ref. [40]). The elemental composition C, H, N, O is reported in Section 3.1 and 3.3. In addition, the light phase contained 0.05% sulfur (wet basis) and 1.72% dissolved metals (mainly K).

Five nickel-based catalysts on various supports and in some cases including promoters were prepared by wet impregnation (details in Ref. [40]): NiCu/Al₂O₃ (17.8% Ni, 2.1% Cu, BET surface 66 m² g⁻¹), Ni/SiO₂ (22.0% Ni, BET surface 170 m² g⁻¹), Ni/ZrO₂ (5.8% Ni, BET surface 110 m² g⁻¹), NiW/AC (3.2% Ni, 7.8% W on Active Carbon, BET surface 1110 m² g⁻¹) and Ni/TiO₂ (5.8% Ni, BET surface 86 m² g⁻¹). The mean Waddell disk diameter of the catalyst particle size was less than 100 μm. A commercial Ni/Al₂O₃ (METH 134 C&CS, nominal loading Ni 20%, Ca 3%, BET surface 76 m² g⁻¹) and Ru/C (Sigma Aldrich, 206180, nominal loading 5%, BET surface 870 m² g⁻¹) were also tested as benchmark.

For the studies with model compounds in water (milliQ), phenol (Merck, 8.22296.1000) and D-glucose monohydrate (Merck, 1.08342.2500) were used. Phenol-d₆ (Aldrich, 176060) and D-glucose-¹³C₆ (Deutero GmbH, 50302) were added to the pyrolysis oil for studies about the reactivity in this medium.

2.2. Hydrodeoxygenation experiments

The experiments were carried out in an Inconel alloy 625 autoclave designed for pressures up to 36 MPa and temperatures up

to 400 °C (manufactured at IKFT-KIT, Fig. S1 of Supporting Information). It was equipped with a magnetically-coupled stirrer (torque 80 N cm, Premex reactor AG) and a gas injection stirrer was employed to facilitate mass transfer of hydrogen in the liquid medium. Heating cartridges inserted in a brass mantle were used for heating and the power supply was controlled by Labview software.

Three kinds of experiment were carried out:

- HDO of the light phase of pyrolysis oil over different nickel-based catalysts or Ru/C: 2.5 g catalyst and circa 50 g light phase were inserted in the autoclave;
- HDO of the light phase of the pyrolysis oil with isotopically labelled molecules over NiCu/Al₂O₃ or Ru/C: 2.5 g catalyst, circa 50 g light phase, 200 μg phenol-d₆ and 200 μg D-glucose-¹³C₆ were inserted in the autoclave. Additional experiments with 10% D-glucose monohydrate in the light phase over NiCu/Al₂O₃ and Ru/C were carried out to gain more information about its reactivity;
- HDO of platform molecules in milliQ water over NiCu/Al₂O₃ or Ru/C: 2.5 g catalyst, 50 g of 10% phenol or D-glucose monohydrate solution were inserted in the autoclave.

A blank test (without catalyst) was carried out for each type of experiment. The results are reported as the average of two experiment replicates. The percentage values indicating concentrations or yields presented in this paper are reported as mass fraction, if not else specified.

Once the reagents were inserted in the autoclave, the autoclave was purged with nitrogen and then pressurized with hydrogen (purity 99.9999%) until 8.0 MPa at room temperature. The stirrer was set at 16.7 Hz and a heating ramp rate of 15 K min⁻¹ was used to reach 340 °C. In this case, the stabilisation of the bio-oil (to avoid polymerization and excessive coke production) was performed during the heating ramp, as reported previously in literature [10,40]. For the sake of comparison, similar reaction conditions to previous literature studies [17,18,41,42] were used. Mass transfer between gas-liquid and liquid-solid phase were minimized using a good mixing (16.7 Hz, gas injection stirrer) and small size of the catalysts grains. The global reaction time including the heating ramp was 100 min. Afterwards the reaction was quenched, first with a flow of compressed air and then with a bath of ice/water. A gas aliquot was sampled and the autoclave was evacuated. The hydrogen consumption was calculated by subtracting the partial pressure of hydrogen at the beginning and end of the reaction (at room temperature) using the Soave-Redlich-Kwong equation as described previously in Ref. [40]. The product mixture was collected and centrifuged at 7240 RCF for 30 min (Thermo Scientific Heraeus Biofuge Stratos, fixed angle rotor 26 n.75003014) to separate the two liquid phases (an aqueous phase and an upgraded oil) and the spent catalyst. The solid was washed with acetone and then dried. To overcome excessive losses in the mass balance, the liquid product yields were calculated using the elemental composition of each phase and the principle that the mass of carbon and oxygen should be conserved during the reaction (equation system below):

$$\begin{cases} \text{Tot C} = (\%wp * C_w + \%oil * C_{oil})/100 \\ \text{Tot O} = (\%wp * O_w + \%oil * O_{oil})/100 \end{cases}$$

Tot C and Tot O are the quantity of carbon and oxygen theoretically recovered from the liquid products. These were calculated by subtracting the respective quantities in gas and solids (oxygen in the solids was considered negligible) from those contained in the original feed. %wp and %oil are the yields (mass fraction expressed as percentage) of aqueous phase and upgraded oil respectively, produced during the reaction. C_w and C_{oil} are the carbon contents

(mass fraction expressed as percentage) determined by elemental analysis of the aqueous and the oil phase, respectively. O_w , O_{oil} is the analogous oxygen content. The yield of the aqueous phase and upgraded oil was obtained solving the system for $\%wp$ and $\%oil$, reducing the mass balance error to less than 3%.

Hydrogen consumption, yield of upgraded oil, deoxygenation degree and van Krevelen plot are reported to estimate and compare the catalyst performance, as shown in other analogous studies [3,16–18].

2.3. Characterization of the products

Four product phases were formed from HDO of the light phase: gases, an upgraded oil (lower density than water), an aqueous phase and coke deposited on the catalyst surface. In the case of model compounds, different product phases were collected depending on the reaction, but the same analytical procedures adopted for the light phase products were used.

The gas composition was characterised by a 7890A Agilent gas chromatograph equipped with two columns (Restek 57096 Hayesep Q and Restek Molsieve 5A) and TCD/FID detectors (for more information, see [Supporting Information](#)).

Different analyses were performed on the two liquid phases. The water content was determined by Karl Fischer titration (Titrand 841 from the company Metrohm.). The elemental analyser CHN628 (Leco) was used to measure carbon, hydrogen and nitrogen content. Oxygen was calculated by difference.

For quantification of phenols and analogous compounds, a GC-FID equipped with a capillary column Type Rxi[®]5Sil MS (0.25 μm \times 0.25 mm \times 30 m) was used. The method and sample preparation is reported in Ref. [40]. A gas chromatograph HP 7980A equipped with a capillary column Stabilwax-DA (Resteck, 0.25 μm \times 0.25 mm \times 30 m) and a FID detector was used for quantification of acids, alcohols, ketones and cyclohexane (for more information, see [Supporting Information](#)). For qualitative analysis, a GC-MS (HP G1800A, GCD system) also with a Stabilwax column was used (for more information, see [Supporting Information](#)).

In order to gain insight about the molecular weight of the components in the bio-oil, gel permeation chromatography (GPC) was performed in a Column-Thermostat T 6300 from Merck provided with a pre-column PSS SDV 5 μm \times 50 mm, two columns PSS SDV 5 μm 1000A 8 \times 300 mm and PSS SDV 5 μm 100A 8 \times 300 mm and a RI-Detector L-7490 from Merck. 10 mg of the sample were dissolved in 5 ml of THF with internal standard toluene.

NMR spectra were measured at 25 °C after diluting the sample 1:10 in CD₃OD with TMSP-d₄ (sodium 3-trimethylsilyl-2,2',3,3'-tetrauteropropionate) as internal reference (~ 2 g L⁻¹). Additional information are available in [Supporting Information](#).

3. Results and discussion

3.1. Hydrogen consumption and hydrotreating mass balance

The main hydrogen consumption took place during the heating ramp. Once the temperature reached 340 °C, only small variations in pressure were recorded. The autogenous pressure reached at the final temperature in the autoclave varied depending on the catalyst used: for the blank experiment the maximum pressure reached was 31 MPa, for Ru/C and NiCu/Al₂O₃ 23 MPa and 25 MPa respectively. Ru/C showed the highest hydrogen consumption at 340 °C ([Table 1](#)). Among the nickel-based catalysts NiCu/Al₂O₃ had a slightly higher activity, enhanced probably by copper promoting the spillover effect [16,43]. In comparison to the previous study at 250 °C [40], hydrotreating at 340 °C resulted in higher H₂ consumption: for example, the use of hydrogen at 340 °C was for Ru/C

21% higher than at 250 °C, for NiCu/Al₂O₃ 23%, for Ni/Al₂O₃ 33%, Ni/ZrO₂ 28%, for Ni/SiO₂ 17%, for NiW/AC 13% and Ni/TiO₂ 5%. Note that different autoclaves were used for the mild and deep HDO studies. A similar study [17] reported a H₂ consumption of 146 L kg_{po}⁻¹ (at normal temperature and pressure, 20 °C and 101.325 kPa) for NiCu/Al₂O₃ and 272 L kg_{po}⁻¹ for Ru/C, in agreement with the results presented in this work normalizing the bio-oil values on dry basis.

Regarding the mass balance, the amount of upgraded oil and aqueous phase produced were comparable among the different experiments and independent of the catalyst used ([Table 1](#)). The upgraded oil yields ranged from 16.8 to 18.2% with respect to the original feed. The upgraded oil contained high concentration of organics with low water content (3–10% depending on the experiment). The aqueous phase constituted a high percentage of the original feed mass, but this was considered a low value fraction with low energy content since 80% \pm 1% was water. Solid and gas formation were negligible in comparison to the liquid products. Material losses were below 3% and were due to the mineral content and the error propagation in elemental analysis and Karl Fischer titration.

100 g of the original light phase of the pyrolysis oil consisted of 20.7 g carbon, 9.5 g hydrogen, 67.8 g oxygen (wet basis, [Table 2](#)) and a small percentage of inorganics. On dry basis, the oil composition was 47.7% C, 7.4% H and 40.0% O. These elements were redistributed in the four phases formed after HDO. On average 60% of the carbon was recovered in the upgraded oil, 33% in the aqueous phase and 6% in the gas ([Table 2](#)). Hydrotreatment in this case was capable of concentrating the majority of carbon in the upgraded oil, densifying the energy content contained in the original feed (HHV 9.2 MJ kg⁻¹) in a smaller volume (upgraded oil HHV 35–37 MJ kg⁻¹). This demonstrates hydrotreatment to be a promising technique for valorization of a low-quality fraction characterised by high water content, sugar derivatives and low heating value, to an upgraded oil which could be further processed for fuel and chemical production.

The majority of the oxygen was present in the aqueous phase, mainly in the form of water (circa 87–89%). The carbon and oxygen content of the organic components in the aqueous phase on dry basis was approximately 44% \pm 1% and 52% \pm 2% respectively. Note that these values should be considered only as an estimation, since the error due to hydrogen measurement of this phase by elemental analysis was not negligible for dry basis. The oxygen content in the upgraded oils was on average 13% \pm 1% (dry basis), in accordance with similar studies [16,17]. The water production related to 100 g of the feed was 7.2 g over Ru/C, in the range of 5.5–5.7 g over nickel catalysts and 5.2 g for the blank experiment ([Table 2](#) and [Table S1](#) of [Supporting Information](#)). Since water was also produced in the blank experiment, this indicates that a fraction was produced directly from thermal/acidic dehydration (not catalyzed by the heterogeneous catalyst), besides HDO and hydrogenation reactions.

The hydrogen mass balance did not close perfectly ([Fig. S2c](#) [Supporting Information](#)), with an average error of 8% in respect to the theoretical value, probably due to the relatively low hydrogen amounts and due to the inherent errors in elemental analysis and Karl Fischer titration. Analogously to oxygen, hydrogen was mainly present as water in the aqueous phase, while more hydrogen was contained in the upgraded oils produced using a catalyst.

3.2. Analysis of the gaseous phase

The main gas detected was CO₂ followed by low amounts of other gases, including methane, ethane and propane, probably as a result of HDO and cracking ([Fig. 1](#)). The blank experiment showed the highest tendency to produce CO₂, which can be formed from decarboxylation or redox reactions among organic molecules

Table 1
Hydrogen consumption, and mass balance (% mass fraction with respect to the original feed amount) of the products of the hydrodeoxygenation reaction over different catalysts (340 °C, 8.0 MPa of hydrogen at room temperature).

	Hydrogen consumption (L/kg)	Upgraded oil (%)	Aqueous phase (%)	Gas (%)	Solid (%)	Loss (%)
blank	12.6 ± 0.8	17.4 ± 0.5	75.6 ± 0.5	4.9 ± 0.3	n.d. ^a	2.3 ± 0.6
Ru/C	130.2 ± 0.9	17.4 ± 0.1	78.0 ± 0.3	3.5 ± 0.1	n.d. ^a	2.3 ± 0.1
Ni/Al ₂ O ₃	82.0 ± 0.3	17.6 ± 0.2	76.2 ± 0.6	3.4 ± 0.1	0.2 ± 0.1	3.3 ± 0.5
NiCu/Al ₂ O ₃	87 ± 4	17.9 ± 0.2	78 ± 2	3.1 ± 0.3	0.1 ± 0.1	2 ± 1
Ni/SiO ₂	68.9 ± 0.1	17.6 ± 0.8	76 ± 1	3.5 ± 0.2	0.3 ± 0.1	2.9 ± 0.1
Ni/ZrO ₂	64 ± 3	17.6 ± 0.5	76.5 ± 0.1	3.6 ± 0.2	0.3 ± 0.1	2.5 ± 0.2
NiW/AC	67.5 ± 0.6	18.2 ± 0.1	76.0 ± 0.5	3.7 ± 0.4	n.d. ^a	2.7 ± 0.1
Ni/TiO ₂	57 ± 3	16.8 ± 0.2	76.8 ± 0.1	3.9 ± 0.1	0.2 ± 0.1	2.7 ± 0.1

^a n.d. = not determined.

Table 2
Elemental composition and other characteristics of the HDO products over different catalysts (340 °C, 8.0 MPa of hydrogen at room temperature).

	Feed [40] ^b	blank	Ru/C	Ni/Al ₂ O ₃	NiCu/Al ₂ O ₃	Ni/SiO ₂	Ni/ZrO ₂	NiW/AC	Ni/TiO ₂
Upgraded oil (wet basis; dry basis)									
C (%)	20.7; 47.7	72.4; 77.4	71.6; 75.7	73.5; 77.1	69.8; 74.9	70.0; 75.1	69.9; 75.5	70.4; 75.6	73.0; 76.8
H (%)	9.5; 7.4	8.2; 8.0	10.5; 10.5	9.5; 9.4	9.8; 9.7	9.2; 9.1	9.1; 8.9	9.4; 9.2	9.1; 9.0
O (%)	67.8; 40.0	18.2; 13.2	16.9; 12.7	15.9; 12.3	19.4; 14.3	19.7; 14.6	20.0; 14.4	19.3; 14.1	16.8; 13.1
N (%)	0.3; 0.7	1.3; 1.3	1.0; 1.1	1.2; 1.2	1.0; 1.1	1.2; 1.2	1.1; 1.1	1.1; 1.1	1.1; 1.2
Water content (%)	56.7	6.6	5.4	4.7	6.8	6.8	7.4	6.9	4.9
Recovered C (%)	—	60.7	60.3	62.5	60.3	59.5	59.5	61.9	59.4
HHV (%)	9.2	35.1	37.5	36.7	36.1	35.4	35.4	35.8	36.0
Aqueous phase (wet basis)									
C (%)	—	8.7	8.9	8.4	9.0	9.0	8.9	8.7	8.9
H (%)	—	10.1	10.5	9.5	10.1	9.5	9.9	9.8	9.8
O (%)	—	81.3	80.7	82.2	80.9	81.5	81.1	81.6	81.4
N (%)	—	—	—	—	—	—	—	—	—
Water content (%)	—	80.2	80.4	80.5	79.0	79.7	79.4	80.2	79.9
Recovered C (%)	—	31.6	33.3	30.8	33.8	33.2	33.0	31.9	32.8
Gases									
C (%)	—	30.0	35.7	36.9	34.2	36.6	35.8	35.7	34.5
H (%)	—	1.0	2.8	3.3	2.6	2.9	2.6	2.5	2.1
O (%)	—	69.1	61.5	59.8	63.2	60.5	61.6	61.8	63.4
Recovered C (%)	—	7.5	6.4	5.9	5.2	6.1	6.2	6.2	6.6
Solids									
C ^a (%)	—	n.d.	n.d.	3.5	2.7	5.4	5.4	n.d.	4.9
Recovered C (%)	—	n.d.	n.d.	0.8	0.7	1.3	1.3	n.d.	1.2
Additional water produced in HDO (%)									
		5.2	7.2	5.7	5.6	5.5	5.5	5.7	5.6

^a Percentage with respect to the catalyst mass.

^b Composition of the light phase.

involving also water. Unsaturated molecules like ethene and propene were detected in the blank experiment, but this amount was minimized over Ru/C and NiCu/Al₂O₃, probably due to the high hydrogenation activity, which converted them to ethane and propane. NiCu/Al₂O₃ showed slightly lower gas production in

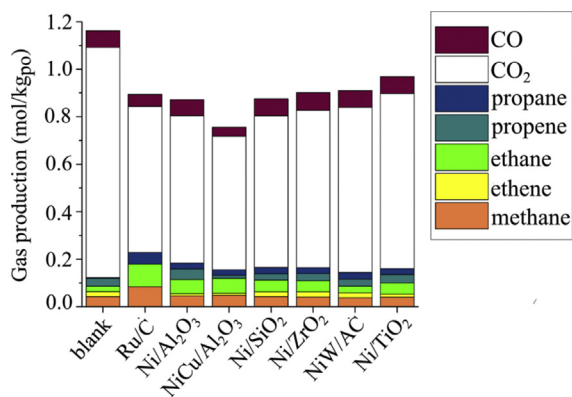


Fig. 1. Gases produced during hydrotreatment over different catalysts during HDO (340 °C, 8.0 MPa H₂ at room temperature).

comparison to the other catalysts. For nickel-based catalysts the quantity of CO₂ appeared inversely proportional to the H₂ consumption. The possibility of CO₂ methanation was excluded, as demonstrated by a previous study [22] using pyrolysis oil in the presence of Ni/Al₂O₃. Therefore, methane formation can be associated more to demethoxylation or demethylation of compounds like guaiacol. This can take place even without a catalyst, since methane was detected also in the blank experiment. The amount of gas produced at 340 °C was on average three times higher compared to the previous experiments at 250 °C [40].

3.3. Characterization of the liquid products

The level of deoxygenation reached was similar for each experiment (68 ± 2%), including the blank experiment, as shown in the van Krevelen plot (dry basis, Fig. 2). On the other hand, the H/C ratio changed considerably depending on the experiment, determining the quality of the upgraded oil. The blank experiment had a low H/C ratio and resulted in a very viscous oil with higher density than water. On the contrary, the upgraded oils obtained using a catalyst had a lower density than the aqueous phase and a viscosity that was apparently lower for higher H/C ratio. The highest H/C ratio was attributed to Ru/C, followed by NiCu/Al₂O₃, in agreement

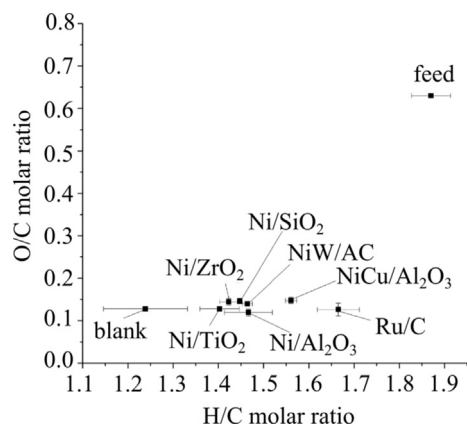


Fig. 2. Van Krevelen plot of the upgraded oils (dry basis) after HDO over different catalysts (340 °C, 8.0 MPa H₂ at room temperature).

with the hydrogen consumption. The Ni-catalysts produced upgraded oils that according to the van Krevelen plot and the GC-MS results were comparable in composition.

Meaningful differences in the chemical composition of the upgraded oils were detected by GC-MS and ¹H-NMR between the blank experiment, Ru/C and NiCu/Al₂O₃ (chosen as representative of the nickel-based catalysts). Ru/C had the highest hydrocarbon production (Fig. 3), forming mainly methylcyclopentane and cyclohexane, identified as HDO products of the sugar derivatives and the lignin fraction respectively. Cyclohexane was produced mainly from HDO of phenol after hydrogenation of the aromatic ring (as reported in Ref. [21]), demonstrated by the presence of intermediates in the HDO products. Methylcyclopentane was formed from HDO of 2-methylcyclopent-2-enone, which was not present in the feed, but probably formed from transformation of sugar derivatives at high temperature and in the acid medium. Specifically, it could derive from the rearrangement of furfural-like compounds into cyclopentanone [8,44–46] and analogous products, which were observed in relatively high concentration in the HDO products. Isomerization of cyclohexane to methylcyclopentane could take place in acid conditions and in the presence of a catalyst [47], but it appeared negligible in this study. NiCu/Al₂O₃ was not active at 340 °C for hydrocarbon production and generally Ni-catalysts formed mostly cyclic ketones (Fig. 3) as observed also by Ardiyanti et al. [16,17]. Cyclohexanone was detected from phenol conversion instead of cyclohexane, and cyclopentanone and 2-methylcyclopentanone were the main products from the sugar derivatives rather than cyclopentane and methylcyclopentane observed over Ru/C (Table 3). Concerning the phenol derivatives, in all experiments guaiacol and syringol were completely converted and no methoxy-groups or other alkoxy-groups bonded to an aromatic unit were observed in the products. Phenol and alkyl-phenols were still detected, demonstrating a lower activity toward HDO of the phenol hydroxyl (Fig. 3c), as reported previously in literature [20,21,48].

The aqueous phase of each experiment contained few organic compounds, especially acids (mainly acetic acid) and alcohols (mainly ethylene glycol, Table 3). In the case of NiCu/Al₂O₃ and Ru/C acetic acid, methyl acetate (esterification product), ethanol, propionic acid, 1,2-ethandiol monoacetate (esterification product) and phenol were detected (propanol was also detected in Ru/C only). For the blank experiment, acetic acid, acetone, methyl acetate, ethanol and 3-methylcyclopent-2-enone were found, together with many unidentifiable compounds. The content of acetic acid was still high in both the aqueous phase and the upgraded oil (Table 3), but

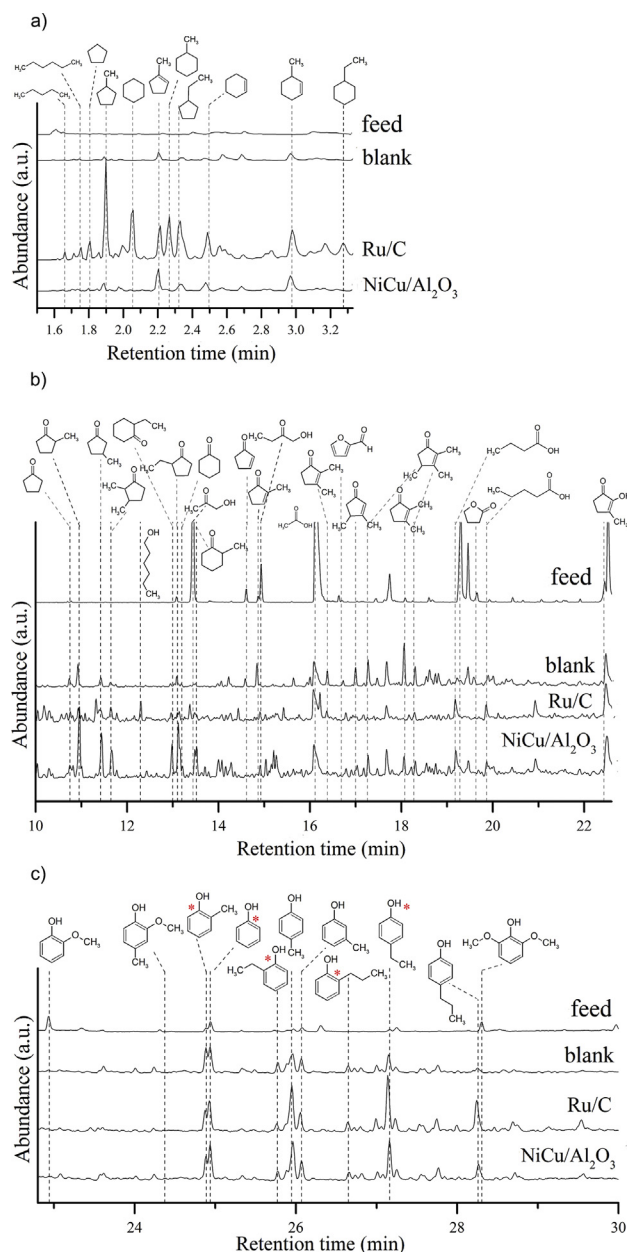


Fig. 3. Typical chromatograms (GC-MS) of the upgraded oils (hydrotreatment at 340 °C, 8.0 MPa H₂ at room temperature) over different catalysts in comparison to the feed (light phase). The chromatograms are divided in 3 regions, where the following components are mainly present: a) hydrocarbons; b) cyclic ketones and acids; c) phenolic derivatives.

the use of a catalyst seemed slightly to reduce this value. Ethylene glycol was recovered mainly in the aqueous phase, but was partially converted, especially over Ru/C (esterification or ethane formation).

Quantitative ¹H-NMR was conducted to gain information about the functional groups present in the products, as reported in Fig. 4. The aromatic groups (8.5–6.0 ppm) were mostly concentrated in the upgraded oil and almost absent in the aqueous phase. Water (or proton-exchanging groups with water, 6.0–4.2 ppm) was the main component in the aqueous phase, but the concentration was relatively low in the upgraded oil. Alcohols (or ether groups, 4.3–3.0 ppm) had a similar concentration in both the aqueous and oil phase, while the concentration of alpha protons to unsaturated groups (3.0–1.5 ppm) was higher for the upgraded oils. The protons

Table 3
Concentration in mass percent (%) of some representative components in the aqueous phase and in the upgraded oils (hydrotreatment at 340 °C, 8.0 MPa of hydrogen at room temperature).

	light phase	blank		Ru/C		NiCu/Al ₂ O ₃	
		upgraded oil	aqueous phase	upgraded oil	aqueous phase	upgraded oil	aqueous phase
Cyclopentanone ^a (%)	n.d.	0.13	0.03	n.d.	n.d.	0.34	0.04
2-methyl-cyclopentanone	n.d.	0.39	0.03	0.08	n.d.	1.41	0.10
phenol ^a (%)	0.11	0.80	0.04	0.69	0.05	0.60	0.04
cyclohexanone ^b (%)	n.d.	n.d.	n.d.	n.d.	n.d.	0.50	n.d.
cyclohexane ^b (%)	n.d.	n.d.	n.d.	0.05	n.d.	n.d.	n.d.
o-kresol ^b (%)	0.04	0.39	n.d.	0.49	n.d.	0.31	n.d.
4-ethylphenol ^b (%)	0.02	0.41	n.d.	0.73	n.d.	0.64	n.d.
acetic acid ^a (%)	4.9	3.49	6.38	3.80	5.24	4.40	5.54
ethylene glycol ^a (%)	7.8	n.d.	5.35	n.d.	1.54	1.02	4.75

^a Analysed by GC equipped with column Stabilwax (0.25 μm × 0.25 mm × 30 m).

^b Analysed by GC equipped with column Type Rxi[®]5Sil MS (0.25 μm × 0.25 mm × 30 m).

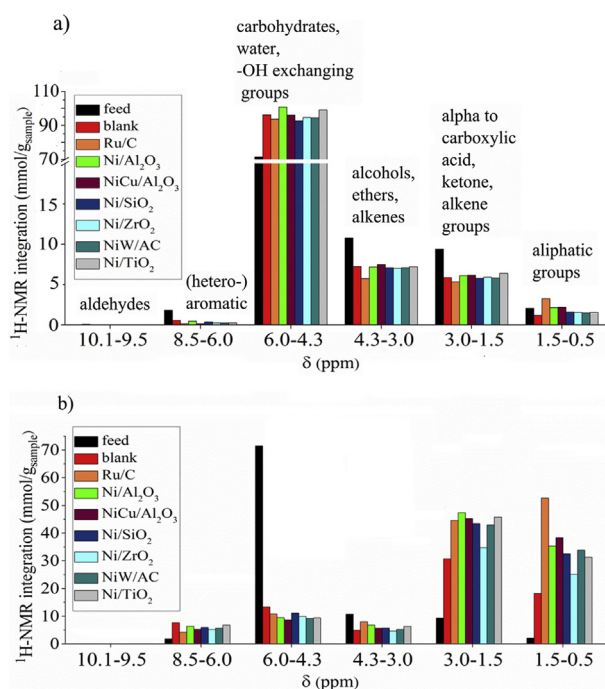


Fig. 4. ¹H-NMR integration of the spectra of the aqueous phases (a) and of the upgraded oils (b) in specific chemical-shift range (hydrotreatment at 340 °C, 8.0 MPa H₂ at room temperature).

of alkane groups (1.5–0.5 ppm) were more prominent in the upgraded oils, and Ru/C had the highest signal, confirming the higher hydrogenation/HDO activity monitored also by GC.

Ru/C had also a slightly inferior concentration of protons in the aromatic region, indicating higher activity towards hydrogenation of the aromatic ring. Ni-catalysts had a similar behavior among them. Only the upgraded oil over Ni/ZrO₂ had a lower concentration of protons, probably due to incomplete solubility in methanol, since the hydrogen content determined by elemental analysis was comparable to the other oils.

In summary, the activity and selectivity of Ru/C and Ni-based catalysts was different in the context of bio-oil resulting in different product classes: over Ni-catalysts mainly ketones, over Ru/C hydrocarbons and alcohols, with low conversion of phenols. Ru/C was therefore more active in HDO and able to hydrogenate the carbonylic groups to alcohols, further to dehydrate the alcohols to olefins and finally hydrogenate the double bond. The selectivity of Ru/C and NiCu/Al₂O₃ (as representative of Ni-catalyst class)

towards these specific product classes was further elucidated by experiments with model compounds in bio-oil and water.

3.4. Reactivity of phenol in aqueous solution and in the pyrolysis oil

The reactivity of phenol, as representative of the lignin fraction, was investigated as a model compound during hydrotreatment in water and in pyrolysis oil (adding phenol-d₆, for identification by GC-MS). Ru/C showed complete conversion of phenol in water with high selectivity to methane (70% of the carbon recovery, Table S2 of Supporting Information). The combination of the temperature, high H₂ pressure and Ru/C promoted hydrocracking instead of HDO. Using NiCu/Al₂O₃, phenol was completely converted to cyclohexane (selectively 85%), cyclohexanol (selectively 15%) and traces of benzene (0.2 g kg⁻¹ in cyclohexane phase). This was in line with the superior gasification activity of Ru compared to Ni reported by Elliott [49].

In contrast, in the light phase of the pyrolysis oil no significant conversion of phenol-d₆ was observed after treatment at 340 °C. For the experiments with unlabelled phenol an average (for the blank experiment, Ru/C and NiCu/Al₂O₃) of 150% ± 10% of the original amount was recovered, probably because additional phenol was produced from lignin derivatives like guaiacol and syringol. Other studies [16,17,31] also reported a significant concentration of phenol or phenolic derivatives in the upgraded oils. In the case of deuterated phenol, an average of 74% ± 2% was still recovered in the blank experiment, over NiCu/Al₂O₃ and Ru/C, demonstrating that it reacted only partially. Furthermore, evidence of proton exchange was observed by GC-MS (Fig. 5a). At 340 °C phenol exchanged the deuterium atoms in the hydroxylic group and in ortho and para position of the aromatic ring with the solvent as an effect of the temperature and the acidic medium. This occurred independent of the presence of a catalyst. The number and positions of atom exchange were determined by a combination of GC-MS and ¹H-NMR respectively (Fig. 5b). The chemical shift at 6.79 and 6.82 ppm (integration 2:1) recorded after an additional experiment at 340 °C using only phenol-d₆ in water, as well as the signal detected in the upgraded oils (a bit shifted and overlapped, Fig. 5b), suggests that the deuterium atoms in the more shielded positions (ortho and para positions, more electronegative for inductive and mesomeric effect) exchanged with protons in the medium (Fig. 5b). The exchange is supposed to happen acid-catalyzed through proton addition and elimination of deuterium, creating as intermediate a carbocation (Fig. 5c). It is important to note that carbocations have the potential to cause polymerization reactions [50], but in this case most of the phenol was recovered. Cyclohexane was produced only over Ru/C in a concentration of 0.5 g kg⁻¹ in the upgraded oil derived from light phase

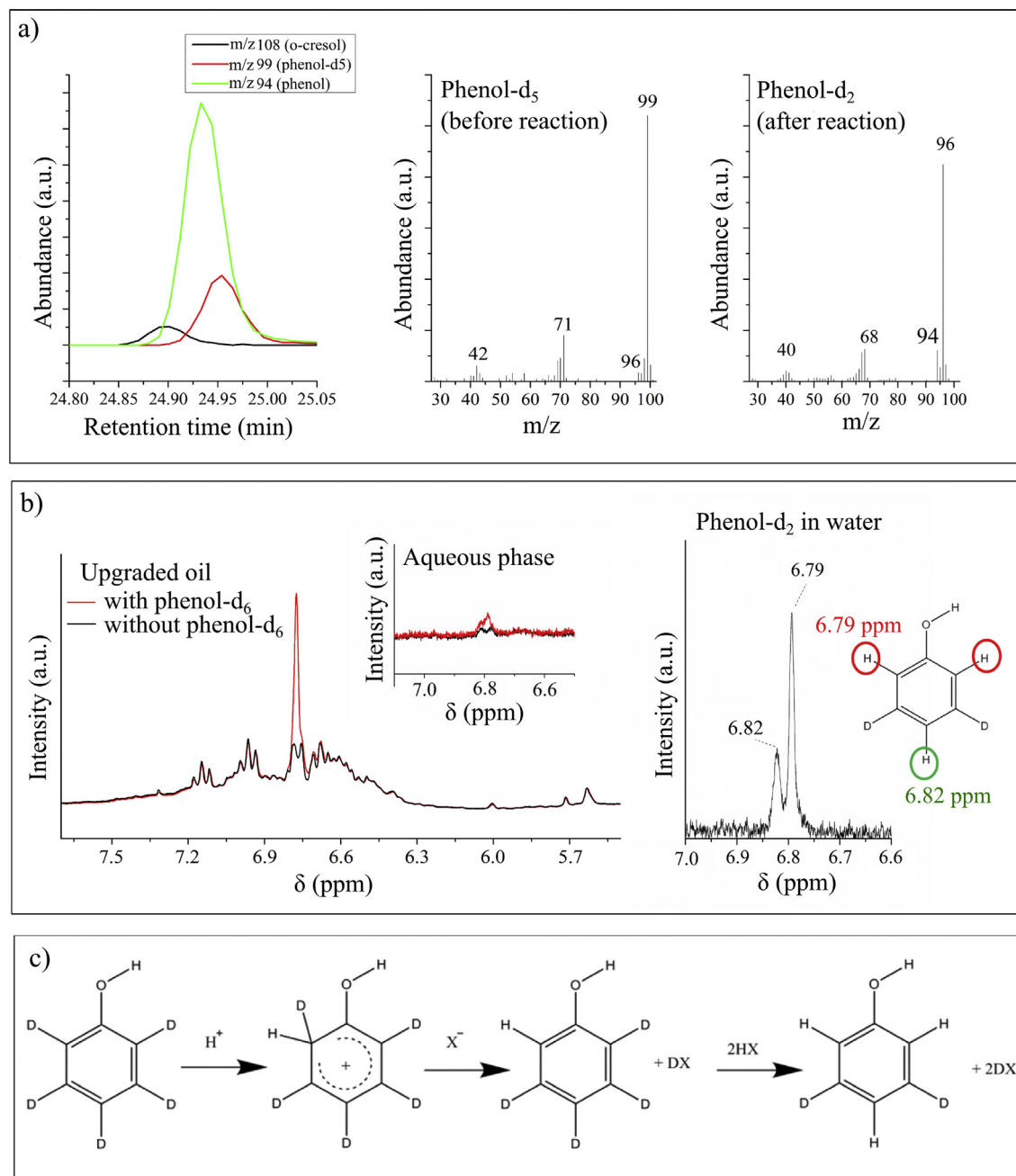


Fig. 5. Reactivity of phenol-d₆ (HDO of light phase at 340 °C, 8.0 MPa H₂ at room temperature). a) Chromatogram (GC-MS) of phenol-d₅ and phenol-d₂ with relative mass spectra. b) Comparison of ¹H-NMR spectra between the upgraded oils (also the aqueous phase) of the blank experiment with and without adding phenol-d₆. Thermal/acidic exchange of deuteriums in ortho and para positions of phenol-d₆. c) Mechanism of the deuterium exchange of phenol-d₅.

hydro-treatment and of 1.1 g kg⁻¹ in the case phenol-d₆ was added. The difference between the two experiments corresponded to around 5% of the starting deuterated phenol. Also the deuterium atoms in meta position were exchanged during the hydrogenation/HDO, as demonstrated in an additional study using only phenol-d₆ in water over NiCu/Al₂O₃ in the same HDO conditions.

One of the reasons for conversion of deuterated phenol, was the formation of a small amount of alkyl-phenols with two mass units higher than the expected molecular weight (2 deuterium remained in the phenol ring). This effect was observed for 2-methyl-phenol, 2-ethyl-phenol, 4-ethyl-phenol and 2-propyl-phenol (Fig. 3c, marked by *) and indicates that C-alkylation occurred between an alcohol and phenol in para and ortho position favored by the acidic

environment of the bio-oil [51,52]. This effect was independent of the catalyst used, since it was also observed in the blank experiment.

3.5. Reactivity of glucose in aqueous solution and in the pyrolysis oil

In contrast to phenol which was hardly converted without a catalyst, D-glucose treated in aqueous solution decomposed spontaneously at high temperature. The blank experiment at 340 °C resulted in no hydrogen consumption producing mainly coke (82.5% mol C) and the remaining components were gaseous. The decomposition of glucose happened already during the heating

ramp (Figure S3 of Supporting Information and reported also in Refs. [53,54]). Over Ru/C as catalyst, D-glucose was completely converted in aqueous solution, producing mainly gases (96.7% mol C, Table S2 of Supporting Information), particularly methane (90% mol C). Similar results were obtained over NiCu/Al₂O₃: 81.9% mol C were recovered in the gas phase (66% methane, Table S2 of Supporting Information), 5.1% in the liquid and 0.7% in the solid (total recovery 87.7%). The conditions and catalysts used appeared to favor hydrocracking instead of HDO, in agreement with earlier studies [55]. During the heating ramp (range 85–130 °C, Fig. S4 of Supporting Information), sorbitol was identified as an intermediate of hydrogenation over both catalysts.

The reactivity of D-glucose-¹³C₆ in pyrolysis oil was monitored by ¹³C-NMR, since this molecule has a typical coupling signal (¹J_{C-C} circa 170–180 Hz, Fig. S5 of Supporting Information) that permits discriminating the signal originated by its conversion products from all others presented in the pyrolysis oil. After the HDO reaction, D-glucose-¹³C₆ was completely converted, but no signals with the specific coupling were detected clearly in the liquid products and no significant differences were noted with the spectra of the experiment without glucose-¹³C₆ (Figure S6 of Supporting Information). The elemental composition also was not affected since the quantity of glucose-¹³C₆ introduced was relatively low. Mass spectra of the gaseous products did not show detectable concentrations of isotopic species. ATR-FTIR of the spent catalysts showed no peak shifts indicating deposition of carbonaceous species derived from the labelled D-glucose. This suggests that probably D-glucose formed a wide range of products at concentrations below the detection limit of the techniques used. In a blank experiment with pyrolysis oil, D-glucose-¹³C₆ was still detected during the heating ramp below 180 °C, but it decomposed at higher temperatures (Figure S7 of Supporting Information).

Since the experiments with small concentration of D-

glucose-¹³C₆ could not elucidate the reaction pathway of this model compound, an alternative experiment using 10% D-glucose monohydrate in pyrolysis oil was carried out in order to increase the derived product concentration. However, this higher amount could modify the matrix and the reactivity of the system, therefore it was not so optimal as using an isotopically-labelled substance. Normalizing the hydrogen consumption for 100 g of pyrolysis oil gave a clear indication about the contribution of the hydrogen consumed by glucose compared to an experiment with only pyrolysis oil. An extra quantity of hydrogen (Table 4) was required when glucose was added equivalent to 1.5 mol H₂ per mol glucose over Ru/C and to 1.0 mol H₂ per mol glucose over NiCu/Al₂O₃. The extra hydrogen was required mainly during the heating ramp after 200 °C with a maximum hydrogen consumption rate at 210 °C (Figure S8 of Supporting Information). Since glucose was converted below 180 °C in the acid environment of the pyrolysis oil, the extra hydrogen consumption should be attributed to hydrogenation/HDO of other species generated from glucose decomposition, probably from dehydration reactions. Generally in the range of 200–230 °C the catalysts were mainly active for hydrogenation reactions [40], therefore hydrogenation of unsaturated groups was more probable than HDO (for example furfural or hydroxymethylfurfural).

The elemental composition of the upgraded oils was not significantly affected by the presence of glucose (Table 4), suggesting that the products formed by glucose had a similar composition to the upgraded oil. In order to highlight any differences, the mass balance was normalized for 100 g of pyrolysis oil, and consequently the mass balance for pyrolysis oil with D-glucose should close to 111 g. Comparing the experiments with and without D-glucose, an increase in the aqueous phase and in the upgraded oil was mainly observed. The increase in the aqueous phase can be mainly traced back to extra production of water (Table 4) and only

Table 4
Main differences between the hydrotreatment experiments without and with addition of glucose (10% in pyrolysis oil at 340 °C. 8.0 MPa H₂ at room temperature). All quantities except elemental analysis are normalized for 100 g of pyrolysis oil (p.o.).

	Ru/C without glucose	Ru/C with glucose	NiCu/Al ₂ O ₃ without glucose	NiCu/Al ₂ O ₃ with glucose
Hydrogen consumption (mol H ₂ /100 g p.o.; L/kg)	0.535 mol/100 g p.o.; 130 L/kg _{p.o.}	0.620 mol/100 g p.o.; 151 L/kg _{p.o.}	0.357 mol/100 g p.o.; 87 L/kg _{p.o.}	0.414 mol/100 g p.o.; 101 L/kg _{p.o.}
Elemental composition (dry basis)				
C content (%)	75.7	76.0	74.9	76.0
H content (%)	10.5	10.0	9.7	9.6
O content (%)	12.7	12.9	14.3	13.4
N content (%)	1.1	1.0	1.1	1.1
Mass balance				
Upgraded oil (%)	17.4	21.5	18.1	22.7
Aqueous phase (%)	78.0	82.8	77.1	81.5
Gas (%)	3.5	4.0	3.1	4.1
Solids (%)	–	–	0.15	0.21
Losses (%)	1.2	2.8	1.7	2.7
Water production for 100 g p.o. (g)				
	7.2	11.3	5.6	10.3
CO ₂ production (mmol for 100 g of p.o.)				
	61	87	56	85
Cyclohexane production (g/L in upgraded oil)				
	0.5	3.4	n.d.	n.d.
Carbon in upgraded oil (%)				
	12.5	15.9	12.5	15.7
Carbon in aqueous phase (%)				
	6.9	7.0	7.0	7.2
Carbon in gas (%)				
	1.3	1.4	1.0	1.4
Oxygen in upgraded oil (%)				
	2.8	3.2	3.5	4.6
Oxygen in aqueous phase (%)				
	62.9	67.7	62.4	66.3
Oxygen in gas (%)				
	2	2.6	1.9	2.6
Hydrogen in upgraded oil (%)				
	1.9	2.2	1.8	2.2
Hydrogen in aqueous phase (%)				
	8.2	8.1	7.9	7.9
Hydrogen in gas (%)				
	0.1	0.1	0.1	0.1

to a few compounds that were water-soluble (see carbon mass balance in Table 4). For 1 mol of glucose an extra production of 3.0 mol water was observed for Ru/C and 3.6 mol for NiCu/Al₂O₃ (1 additional water mol came from the feedstock since glucose monohydrate was used). Therefore D-glucose was converted into molecules with a lower amount of oxygen, as observed also in the upgraded oil composition (Table 4). Oxygen from glucose was mainly distributed in the aqueous phase in form of water, carbon in the upgraded oil, while errors associated with the hydrogen mass balance did not permit further conclusions. The quantity of the gaseous products was slightly higher when glucose was used, and the main contribution was due to extra production of CO₂ (circa 0.5 mol CO₂ per mol of glucose). Solid formation was difficult to monitor with Ru/C, since similar amounts of catalyst were recovered at the start and end of the reaction. For NiCu/Al₂O₃ a negligible higher amount of carbon was detected on the surface of the catalyst (Table 4). In conclusion D-glucose was converted to different components that were mainly distributed in the upgraded oil. The carbon recovery of glucose in the different phases was: 85.0% in the upgraded oil, 7.7% in the gas, 2.5% in the aqueous phase for Ru/C; 80.0% in the upgraded oil, 8.6% in the gas, 5.0% in the aqueous phase for NiCu/Al₂O₃.

By normalizing the ¹H-NMR spectrum per 100 g of pyrolysis oil and comparing the experiment with and without glucose, the main contribution due to glucose was shown in the alkane region (0.5–1.5 ppm, more intense for Ru/C than NiCu/Al₂O₃) and by the alpha protons to carboxylic, ketones and unsaturated groups (1.5–3.0 ppm) (Fig. 6a and b). No contributions came from the aromatic region and neither from the alcohols (the single peak at

3.3 ppm is due to the deuterated solvent). This is in agreement with the elemental mass balance, affirming that glucose products should have a lower oxygen content.

Similar compounds were detected by GC-MS and GC-FID in the experiments with and without glucose over Ru/C, but their concentrations were slightly different. In the first region of the chromatogram (5–7 min, Fig. 7) alkanes, such as cyclohexane and methylcyclopentane, and alkenes were detected in higher concentration in the experiment with glucose. The concentration of cyclohexane in the upgraded oil produced over Ru/C was 3.4 g L⁻¹ for the experiment with glucose, whereas it was only 0.5 g L⁻¹ for the experiment without additional glucose. However, the extra amount of cyclohexane produced corresponded only to 1.4% mol of the initial carbon mols of D-glucose. In the case of NiCu/Al₂O₃, the chromatograms were similar and no big differences were detected, indicating that no extra hydrocarbons were formed (Figure S9 of Supporting Information). The addition of glucose resulted in producing mainly higher molecular-weight compounds, which were not detectable by GC, but only by GPC, as reported in Fig. 8 for NiCu/Al₂O₃. They can stem from the polymerization of intermediate decomposition products of D-glucose (as indicated in some reaction pathways reported in Ref. [56]) and from the parallel HDO. In summary, a vast amount of liquid products not easily identifiable and below the ¹³C-NMR detection limit were produced from D-glucose over both catalysts. This shows that in contrast to phenol, characterizing and understanding the reactivity of sugar derivatives in pyrolysis oil is more of a challenge. Not many studies have been addressed to this fraction yet [32,56–58] and usually they were carried out at lower temperature, finding a complex mixture of

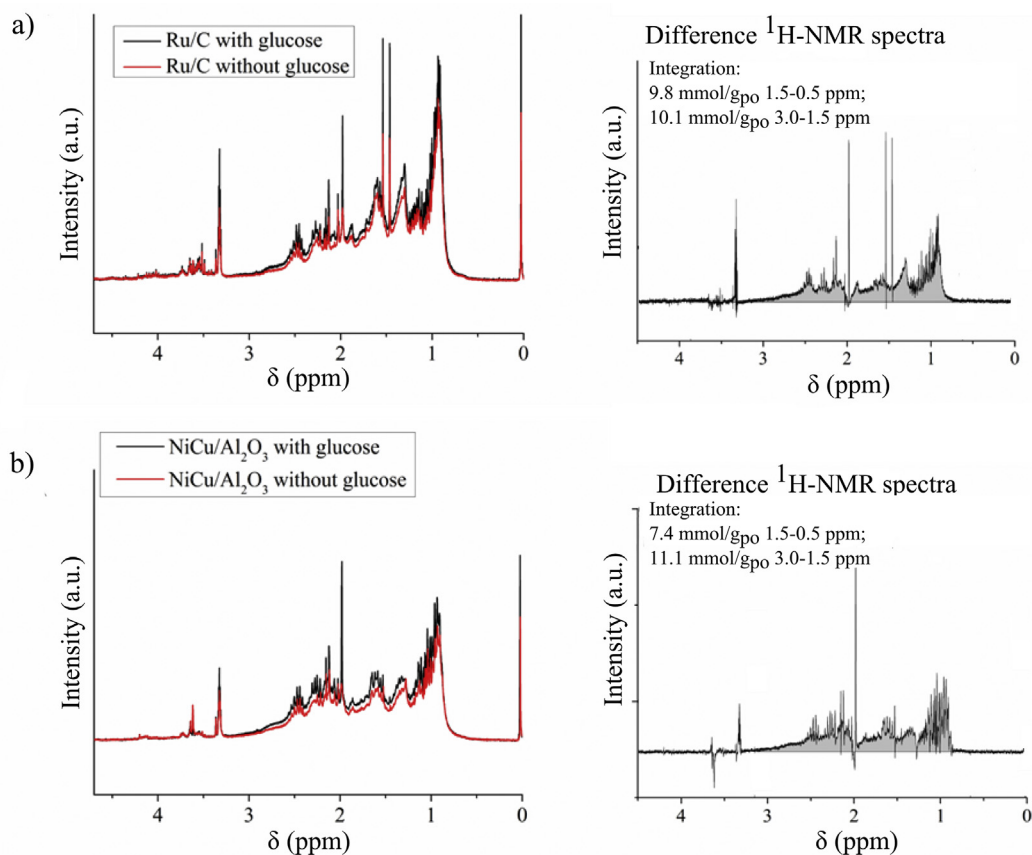


Fig. 6. a) Comparison of ¹H-NMR spectra of the upgraded oils produced over Ru/C (a) and NiCu/Al₂O₃ (b) without and with addition of glucose (10% in pyrolysis oil, at 340 °C, 8.0 MPa H₂ at room temperature); on the left comparison of the spectra normalized for 100 g light phase; on the right difference of the signal between the two spectra.

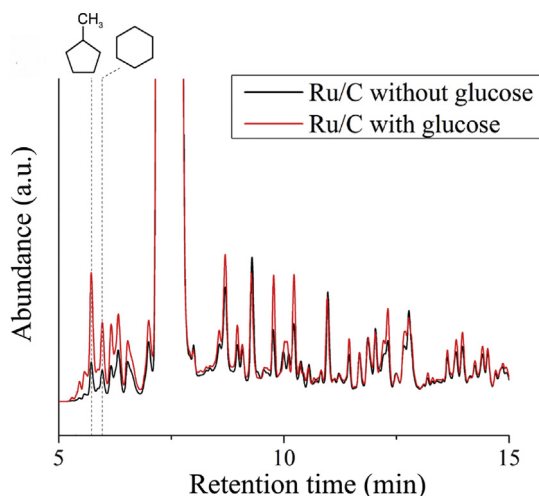


Fig. 7. Comparison of the chromatograms (GC-FID, column Stabilwax) of upgraded oils from the hydrotreatment experiments over Ru/C without and with addition of glucose (10% in pyrolysis oil, at 340 °C, 8.0 MPa H₂ at room temperature).

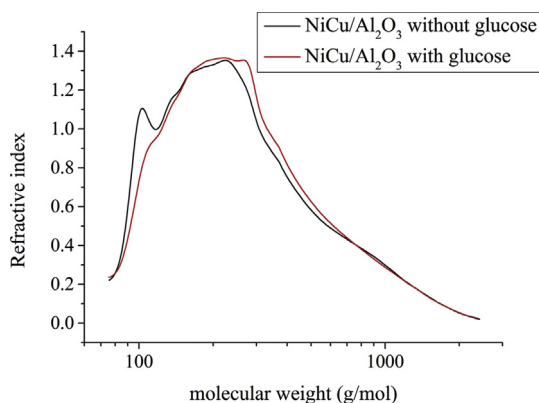


Fig. 8. Comparison of the gel permeation chromatograms (GPC) of upgraded oils from the hydrotreatment experiments over NiCu/Al₂O₃ without and with addition of glucose (10% in pyrolysis oil, at 340 °C, 8.0 MPa H₂ at room temperature).

products mainly constituted by alcohols and polyols.

3.6. Analysis of the catalysts after hydrotreatment

Pyrolysis oil contains several components of organic and inorganic nature that can deactivate the catalyst. Therefore the catalysts were analysed after the reaction to gain information on their stability and robustness. A more detailed analysis of the catalysts has recently been reported [59] and which is in line with observations in this publication. Elemental analysis showed that carbon deposits were present on the catalyst surface (range 2.7–5.4%), probably due to the polymerization of bio-oil components at high temperature and in acid environment. For catalysts supported on activated carbon the solid content could not be determined by elemental analysis or by difference in weight. Nitrogen and sulfur were detected in the catalyst by elemental analysis (0.1–0.9%), together with various inorganic elements detected by SEM-EDX: sulfur 0.6–1.4%, calcium 1.4–4.5%, potassium 0.2–1.1%, chlorine 0–0.4%, phosphorus 0.6–1.2%, magnesium 0.2–1.8%. Leaching of the active metal was limited to low amounts (less than 0.4%).

The XRD patterns of the spent catalysts showed in some cases besides the presence of metallic nickel, small reflections due to Ni₃S₂. An increase in Ni particle size was also observed [59]. The

crystalline structure of NiW/AC was strongly affected by the presence of calcium (concentration of 2.2 g kg⁻¹ in the feed), converting tungsten oxide completely into CaWO₄.

The significant changes detected on the catalyst after the reaction, especially the formation of Ni₃S₂, can explain the different behavior of the platform molecules in the two different media. While sulfur is difficult to eliminate from the bio-oil, the mineral content could be reduced improving the catalyst performance by leaching of the biomass as pre-treatment to pyrolysis or by hot vapor filtration during the fast pyrolysis process [5]. Further studies will be addressed to the hydrotreatment of filtered pyrolysis oils and to a deep characterization of the catalyst deactivation on long terms.

4. Conclusions

In this work, a set of nickel catalysts was tested in the context of hydrodeoxygenation of the light phase of bio-oil and showed distinct differences to the performance of a commercial Ru/C catalyst. In addition, the reaction medium (pyrolysis oil vs. water) had a strong influence on the activity and selectivity of the catalyst.

Nickel-based catalysts and Ru/C are suitable for HDO of the light phase of pyrolysis oil, forming upgraded oils with lower oxygen and higher energy content compared to the feed. The treatment of a feed which contains a high percentage of water and sugar derivatives demonstrated that it is also possible to valorise low value educts, which are normally considered as waste, and to recover the main carbon content of the feed in the upgraded oil. Hydrotreatment of the pyrolysis oil over Ni catalyst produced upgraded oils with high ketone content, whereas over Ru/C hydrocarbon and alcohol formation was observed. Phenolic compounds were not significantly converted by any of the catalysts tested. The different results obtained during HDO of phenol and D-glucose in water and pyrolysis oil demonstrate that the complex bio-oil composition influences both the reactivity of the model compounds and the catalyst activity. Coke and inorganic deposits, especially sulfur modify the catalyst activity. Therefore, purification of the feed is required before hydrotreatment (e.g. hot vapor filtration) or alternatively catalysts that are more resistant to poisoning.

Future studies related to hydrodeoxygenation of model compounds should consider the influence of poisoning, how the catalyst selectivity is changed and if the modified activity of the catalyst can be used as an advantage to produce fine chemicals. In order to optimise the process and obtain lower oxygen content in the upgraded oils, continuous reactors should be employed for nickel-based catalysts. Additional studies should thus focus on understanding catalyst deactivation during long-term use in the bio-oil in a continuous reactor.

Acknowledgments

The authors would like to thank Saint Gobain NorPro for supplying the catalyst supports and the Helmholtz Research School Energy-Related Catalysis (VH-KO-403) for financial support. For technical assistance and measurements at IKFT-KIT we thank B. Rolli, G. Zwick, H. Köhler, J. Maier, P. Janke, J. Heinrich, P. Griesheimer and T. Zevaco. Furthermore, we acknowledge discussions with T. Sheppard.

Appendix A. Supplementary data

Supplementary data related to this article can be found at <http://dx.doi.org/10.1016/j.biombioe.2017.08.013>.

References

- [1] W.P.M. van Swaaij, S.R.A. Kersten, W. Palz, Biomass Power for the World, CRC Press, 2015.
- [2] G.W. Huber, S. Iborra, A. Corma, Synthesis of transportation fuels from Biomass: chemistry, catalysis, and engineering, *Chem. Rev.* 106 (2006) 4044–4098.
- [3] P.M. Mortensen, J.-D. Grunwaldt, P.A. Jensen, K.G. Knudsen, A.D. Jensen, A review of catalytic upgrading of bio-oil to engine fuels, *Appl. Catal. A* 407 (2011) 1–19.
- [4] A.H. Zacher, M.V. Olarte, D.M. Santos, D.C. Elliott, S.B. Jones, A review and perspective of recent bio-oil hydrotreating research, *Green Chem.* 16 (2014) 491–515.
- [5] A.V. Bridgwater, Review of fast pyrolysis of biomass and product upgrading, *Biomass Bioenergy* 38 (2012) 68–94.
- [6] D.C. Elliott, Historical developments in hydroprocessing bio-oils, *Energy Fuels* 21 (2007) 1792–1815.
- [7] D.A. Bulushev, J.R.H. Ross, Catalysis for conversion of biomass to fuels via pyrolysis and gasification: a review, *Catal. Today* 171 (2011) 1–13.
- [8] D.C. Elliott, Biofuel from fast pyrolysis and catalytic hydrodeoxygenation, *Curr. Opin. Chem. Eng.* 9 (2015) 59–65.
- [9] D.C. Elliott, Transportation fuels from biomass via fast pyrolysis and hydroprocessing, *Wiley Interdiscip. Rev. Energy Environ.* 2 (2013) 525–533.
- [10] F. de Miguel Mercader, M.J. Groeneveld, S.R.A. Kersten, N.W.J. Way, C.J. Schaverien, J.A. Hogendoorn, Production of advanced biofuels: Co-processing of upgraded pyrolysis oil in standard refinery units, *Appl. Catal. B* 96 (2010) 57–66.
- [11] S. Arbogast, D. Bellman, J.D. Paynter, J. Wykowski, Advanced biofuels from pyrolysis oil... Opportunities for cost reduction, *Fuel Process. Technol.* 106 (2013) 518–525.
- [12] E. Furimsky, Catalytic hydrodeoxygenation, *Appl. Catal. A* 199 (2000) 147–190.
- [13] E. Furimsky, Hydroprocessing challenges in biofuels production, *Catal. Today* 217 (2013) 13–56.
- [14] Z. Ma, L. Wei, W. Zhou, L. Jia, B. Hou, D. Li, Y. Zhao, Overview of catalyst application in petroleum refinery for biomass catalytic pyrolysis and bio-oil upgrading, *Rsc Adv.* 5 (2015) 88287–88297.
- [15] V.A. Yakovlev, S.A. Khromova, O.V. Sherstyuk, V.O. Dundich, D.Y. Ermakov, V.M. Novopashina, M.Y. Lebedev, O. Bulavchenko, V.N. Parmon, Development of new catalytic systems for upgraded bio-fuels production from bio-crude-oil and biodiesel, *Catal. Today* 144 (2009) 362–366.
- [16] A.R. Ardiyanti, M.V. Bykova, S.A. Khromova, W. Yin, R.H. Venderbosch, V.A. Yakovlev, H.J. Heeres, Ni-based catalysts for the hydrotreatment of fast pyrolysis oil, *Energy Fuels* 30 (3) (2016) 1544–1554.
- [17] A.R. Ardiyanti, S.A. Khromova, R.H. Venderbosch, V.A. Yakovlev, H.J. Heeres, Catalytic hydrotreatment of fast-pyrolysis oil using non-sulfided bimetallic Ni–Cu catalysts on a δ -Al₂O₃ support, *Appl. Catal. B* 117–118 (2012) 105–117.
- [18] A.R. Ardiyanti, S.A. Khromova, R.H. Venderbosch, V.A. Yakovlev, I.V. Melián-Cabrera, H.J. Heeres, Catalytic hydrotreatment of fast pyrolysis oil using bimetallic Ni–Cu catalysts on various supports, *Appl. Catal. A* 449 (2012) 121–130.
- [19] M.V. Bykova, D.Y. Ermakov, S.A. Khromova, A.A. Smirnov, M.Y. Lebedev, V.A. Yakovlev, Stabilized Ni-based catalysts for bio-oil hydrotreatment: reactivity studies using guaiacol, *Catal. Today* 220–222 (2014) 21–31.
- [20] M.V. Bykova, D.Y. Ermakov, V.V. Kaichev, O.A. Bulavchenko, A.A. Saraev, M.Y. Lebedev, V.A. Yakovlev, Ni-based sol–gel catalysts as promising systems for crude bio-oil upgrading: guaiacol hydrodeoxygenation study, *Appl. Catal. B* 113–114 (2012) 296–307.
- [21] P.M. Mortensen, J.-D. Grunwaldt, P.A. Jensen, AnD. Jensen, Screening of catalysts for hydrogenation of phenol as a model compound for bio-oil, *ACS Catal.* (2013) 1774–1785.
- [22] W. Olbrich, C. Boscagli, K. Raffelt, H. Zang, N. Dahmen, J. Sauer, Catalytic hydrodeoxygenation of pyrolysis oil over nickel-based catalysts under H₂/CO₂ atmosphere, *Sustain. Chem. Process* (2016) 4–9.
- [23] V.A. Yakovlev, M.V. Bykova, S.A. Khromova, Stability of nickel-containing catalysts for hydrodeoxygenation of biomass pyrolysis products, *Catal. Ind.* 4 (2012) 324–339.
- [24] M.V. Bykova, O.A. Bulavchenko, D.Yu Ermakov, M.Yu Lebedev, V.A. Yakovlev, V.N. Parmon, Guaiacol hydrodeoxygenation in the presence of Ni-containing catalysts, *Catal. Ind.* 3 (2011) 15–22.
- [25] M.V. Bykova, S.G. Zavarukhin, L.I. Trusov, V.A. Yakovlev, Guaiacol hydrodeoxygenation kinetics with catalytic deactivation taken into consideration, *Kinet. Catal.* 54 (2013) 40–48.
- [26] S. Echeandia, P.L. Arias, V.L. Barrio, B. Pawelec, J.L.G. Fierro, Synergy effect in the HDO of phenol over Ni–W catalysts supported on active carbon: effect of tungsten precursors, *Appl. Catal. B* 101 (2010) 1–12.
- [27] C. Zhao, Y. Kou, A.A. Lemonidou, X. Li, J.A. Lercher, Hydrodeoxygenation of bio-derived phenols to hydrocarbons using RANEY® Ni and Nafion/SiO₂ catalysts, *Chem. Commun.* 46 (2010) 412–414.
- [28] Z. He, X. Wang, Hydrodeoxygenation of model compounds and catalytic systems for pyrolysis bio-oils upgrading, *Catal. Sustain. Energy* 1 (2012) 28–52.
- [29] R.H. Venderbosch, A.R. Ardiyanti, J. Wildschut, A. Oasmaa, H.J. Heeres, Stabilization of biomass-derived pyrolysis oils, *J. Chem. Technol. Biotechnol.* 85 (2010) 674–686.
- [30] H.P.R. Kannapu, C.A. Mullen, Y. Elkasabi, A.A. Boateng, Catalytic transfer hydrogenation for stabilization of bio-oil oxygenates: reduction of p-cresol and furfural over bimetallic Ni–Cu catalysts using isopropanol, *Fuel Process. Technol.* 137 (2015) 220–228.
- [31] X. Zhang, J. Long, W. Kong, Q. Zhang, L. Chen, T. Wang, L. Ma, Y. Li, Catalytic upgrading of bio-oil over Ni-Based catalysts supported on mixed oxides, *Energy Fuels* 28 (2014) 2562–2570.
- [32] M. Zhou, G. Xiao, K. Wang, J. Jiang, Catalytic conversion of aqueous fraction of bio-oil to alcohols over CNT-supported catalysts, *Fuel* 180 (2016) 749–758.
- [33] M. Hellinger, H.W.P. de Carvalho, S. Baier, L. Gharnati, J.-D. Grunwaldt, Solvent influence on the hydrodeoxygenation of guaiacol over Pt/SiO₂ and Pt/H-MFI90 catalysts, *Chem. Ing. Tech.* 87 (2015) 1771–1780.
- [34] A.A. Dwiannoko, S. Lee, H.C. Ham, J.-W. Choi, D.J. Suh, J.-M. Ha, Effects of carbohydrates on the hydrodeoxygenation of lignin-derived phenolic compounds, *ACS Catal.* 5 (2015) 433–437.
- [35] F. de Miguel Mercader, P.J.J. Koehorst, H. J. Heeres, S.R.A. Kersten, J.A. Hogendoorn, Competition between hydrotreating and polymerization reactions during pyrolysis oil hydrodeoxygenation, *AIChE J.* 57 (2011) 3160–3170.
- [36] E. Furimsky, F.E. Massoth, Deactivation of hydroprocessing catalysts, *Catal. Today* 52 (1999) 381–495.
- [37] P.M. Mortensen, D. Gardini, H.W.P. de Carvalho, C.D. Damsgaard, J.-D. Grunwaldt, P.A. Jensen, J.B. Wagner, A.D. Jensen, Stability and resistance of nickel catalysts for hydrodeoxygenation: carbon deposition and effects of sulfur, potassium, and chlorine in the feed, *Catal. Sci. Technol.* 4 (2014) 3672–3686.
- [38] R.S. Weber, M.V. Olarte, H. Wang, Modeling the kinetics of deactivation of catalysts during the upgrading of bio-oil, *Energy Fuels* 29 (2015) 273–277.
- [39] N. Dahmen, E. Dinjus, T. Kolb, U. Arnold, H. Leibold, R. Stahl, State of the art of the bioliq® process for synthetic biofuels production, *Environ. Prog. Sustain. Energy* 31 (2012) 176–181.
- [40] C. Boscagli, K. Raffelt, T.A. Zevaco, W. Olbrich, T.N. Otto, J. Sauer, J.-D. Grunwaldt, Mild hydrotreatment of the light fraction of fast-pyrolysis oil produced from straw over nickel-based catalysts, *Biomass Bioenergy* 83 (2015) 525–538.
- [41] J. Wildschut, M. Iqbal, F.H. Mahfud, I.M. Cabrera, R.H. Venderbosch, H.J. Heeres, Insights in the hydrotreatment of fast pyrolysis oil using a ruthenium on carbon catalyst, *Energy Environ. Sci.* 3 (2010) 962–970.
- [42] J. Wildschut, F.H. Mahfud, R.H. Venderbosch, H.J. Heeres, Hydrotreatment of fast pyrolysis oil using heterogeneous noble-metal catalysts, *Ind. Eng. Chem. Res.* 48 (2009) 10324–10334.
- [43] Y. Yao, D.W. Goodman, Direct evidence of hydrogen spillover from Ni to Cu on Ni–Cu bimetallic catalysts, *J. Mol. Catal. Chem.* 383–384 (2014) 239–242.
- [44] R. Fang, H. Liu, R. Luque, Y. Li, Efficient and selective hydrogenation of biomass-derived furfural to cyclopentanone using Ru catalysts, *Green Chem.* 17 (2015) 4183–4188.
- [45] Y. Yang, Z. Du, Y. Huang, F. Lu, F. Wang, J. Gao, J. Xu, Conversion of furfural into cyclopentanone over Ni–Cu bimetallic catalysts, *Green Chem.* 15 (2013) 1932–1940.
- [46] G. Li, N. Li, X. Wang, X. Sheng, S. Li, A. Wang, Y. Cong, X. Wang, T. Zhang, Synthesis of diesel or jet fuel range cycloalkanes with 2-methylfuran and cyclopentanone from lignocellulose, *Energy Fuels* 28 (2014) 5112–5118.
- [47] R.K.M.R. Kallury, T.T. Tidwell, D.G.B. Boocock, D.H.L. Chow, High temperature catalytic hydrogenolysis and alkylation of anisole and phenol, *Can. J. Chem.* 62 (1984) 2540–2545.
- [48] S.A. Khromova, M.V. Bykova, O.A. Bulavchenko, D.Y. Ermakov, A.A. Saraev, V.V. Kaichev, R.H. Venderbosch, V.A. Yakovlev, Furfural hydrogenation to furfuryl alcohol over bimetallic Ni–Cu sol–gel catalyst: a model reaction for conversion of oxygenates in pyrolysis liquids, *Top. Catal.* (2016) 1–11.
- [49] D.C. Elliott, Catalytic hydrothermal gasification of biomass, *Biofuels Bioprod. Biorefining* 2 (2008) 254–265.
- [50] C.H. Bartholomew, Mechanisms of catalyst deactivation, *Appl. Catal. A* 212 (2001) 17–60.
- [51] L. Nie, D.E. Resasco, Improving carbon retention in biomass conversion by alkylation of phenolics with small oxygenates, *Appl. Catal. A* 447–448 (2012) 14–21.
- [52] T.N. Pham, D. Shi, D.E. Resasco, Evaluating strategies for catalytic upgrading of pyrolysis oil in liquid phase, *Appl. Catal. B* 145 (2014) 10–23.
- [53] Y. Matsumura, S. Yanachi, T. Yoshida, Glucose decomposition kinetics in water at 25 MPa in the temperature range of 448–673 K, *Ind. Eng. Chem. Res.* 45 (6) (2006) 1875–1879.
- [54] Q. Jing, X. Lü, Kinetics of non-catalyzed decomposition of glucose in high-temperature liquid water, *Chin. J. Chem. Eng.* 16 (2008) 890–894.
- [55] K. Murata, M. Inaba, I. Takahara, Y. Liu, Selective hydrocarbon production by the hydrocracking of glucose, *React. Kinet. Mech. Catal.* 110 (2013) 295–307.
- [56] J. Wildschut, J. Arentz, C.B. Rasrendra, R.H. Venderbosch, H.J. Heeres, Catalytic hydrotreatment of fast pyrolysis oil: model studies on reaction pathways for the carbohydrate fraction, *Environ. Prog. Sustain. Energy* 28 (2009) 450–460.
- [57] F. de Miguel Mercader, M.J. Groeneveld, S.R.A. Kersten, C. Geantet, G. Toussaint, N.W.J. Way, C.J. Schaverien, K.J.A. Hogendoorn, Hydrodeoxygenation of pyrolysis oil fractions: process understanding and quality assessment through co-processing in refinery units, *Energy Environ. Sci.* 4 (2011) 985–997.
- [58] A. Sanna, T.P. Vispute, G.W. Huber, Hydrodeoxygenation of the aqueous fraction of bio-oil with Ru/C and Pt/C catalysts, *Appl. Catal. B* 165 (2015) 446–456.
- [59] C. Boscagli, C. Yang, A. Welle, W. Wang, S. Behrens, K. Raffelt, J.-D. Grunwaldt, Effect of pyrolysis oil components on the activity and selectivity of nickel-based catalysts during hydrotreatment, *Appl. Catal. A* 544 (2017) 161–172.